Spectrochimica Acta Part A 74 (2009) 78–83

Contents lists available at ScienceDirect

Spectrochimica Acta Part A: Molecular and Biomolecular Spectroscopy

journal homepage: www.elsevier.com/locate/saa

Synthesis, growth, spectral, thermal, mechanical and optical properties of 4-chloro-4′dimethylamino-benzylidene aniline crystal: A third order nonlinear optical material

S. Leela[a], K. Ramamurthi[a,*], G. Bhagavannarayana[b]

[a] Crystal Growth and Thin Film Laboratory, School of Physics, Bharathidasan University, Tiruchirappalli 620024, Tamil Nadu, India
[b] Materials Characterization Division, National Physical Laboratory, Dr. K.S. Krishnan Marg, New Delhi 110012, India

ARTICLE INFO

Article history:
Received 29 November 2008
Received in revised form 24 April 2009
Accepted 13 May 2009

PACS:
81.10.Dn
61.66.H
65.60

Keywords:
Solution growth
Organic compounds
Powder diffraction
Nuclear magnetic resonance
Nonlinear optical materials

ABSTRACT

An organic nonlinear optical material, 4-chloro-4′dimethylamino-benzylidene aniline (CDMABA), was synthesized by the condensation of the p-chloroaniline and p-dimethylaminobenzaldehyde. Solubility of CDMABA was determined in acetone at different temperatures. Single crystals were grown by the solvent evaporation method from acetone solution at room temperature. Grown crystal was subjected to FTIR, FT-Raman and ^{1}H NMR spectral analyses to confirm the synthesized compound. The range and percentage of optical transmission was ascertained by recording UV–vis–NIR spectrum. Thermal properties were investigated by Thermo Gravimetric, Differential Thermal and Differential Scanning Calorimetric analyses. High Resolution X-ray Diffractometry (HRXRD) was employed to evaluate the perfection of the grown crystal. The third order nonlinear optical parameters (nonlinear refractive index and nonlinear absorption coefficient) were derived by the Z-scan technique.

1. Introduction

Search for new materials with high optical nonlinearities has been the important task because of their practical application in harmonic generation, amplitude and phase modulation, switching and other signal processing devices [1–3]. An ultimate goal for designing the molecules with large third order nonlinearities is to incorporate them into devices used in all optical signals processing [4,5]. Nonlinear optical absorption (NOA) has shown its potential application in optical information storage, all optical logic gates, laser radiation protection, and locked laser mode. Interest in searching for NOA materials has been gradually increased [6]. Organic molecules have been the subjects of great attention due to their potential applications in nonlinear optics (NLO), optical switching, and light emitting diodes. Indeed, the potential use of organic device materials in optoelectronics is now a very serious matter [7]. Organic compounds formed by the condensation of primary amines with aldehydes or ketones yield Schiff bases containing imine (C=N) functional group [8]. Some of these compounds are donor–acceptor benzene derivatives, which conform the conjugated π-electron systems and exhibit extremely large second order optical nonlinearities, such as 4-nitro-4′methyl benzylidene aniline (NMBA) [9] and 4-nitro-4′methoxy benzylidene aniline (NMOBA) [10]. Benzylidene anilines constitute an important class of Schiff bases that have been widely used in coordinate, medical and biological chemistry. They possess significant anticancer and anti-inflammatory activities and may also serve as reagents for stereo selective organic synthesis [11]. Recently, the thermochromism, photochromism and nonlinear optical properties of the Schiff base compounds find applications in modern technologies. The structure of the CDMABA compound was studied by You et al. and the space group of the compound is $P2_1/c$ [12]. However, to our knowledge no systematic studies on the growth and characterization of 4-chloro-4′dimethylamino-benzylidene aniline (CDMABA) have been made. Hence in the present work systematic studies on the growth and structural, optical, thermal, mechanical and third order nonlinear optical properties of 4-chloro-4′dimethylamino-benzylidene aniline are reported.

2. Experiment

2.1. Material synthesis and purification

CDMABA was synthesized by the condensation reaction between 4-dimethylaminobenzaldehyde (p-DMAB) and 4-chloro-

---

* Corresponding author. Tel.: +91 431 2407057; fax: +91 431 2407045.
E-mail address: krmurthin@yahoo.co.in (K. Ramamurthi).

1386-1425/$ – see front matter © 2009 Elsevier B.V. All rights reserved.
doi:10.1016/j.saa.2009.05.028

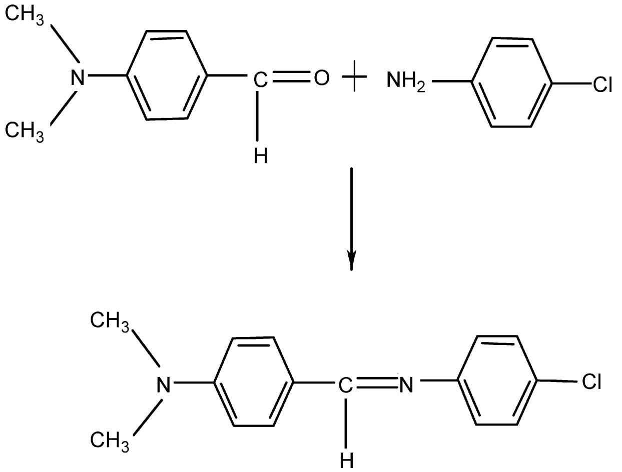

Scheme 1.

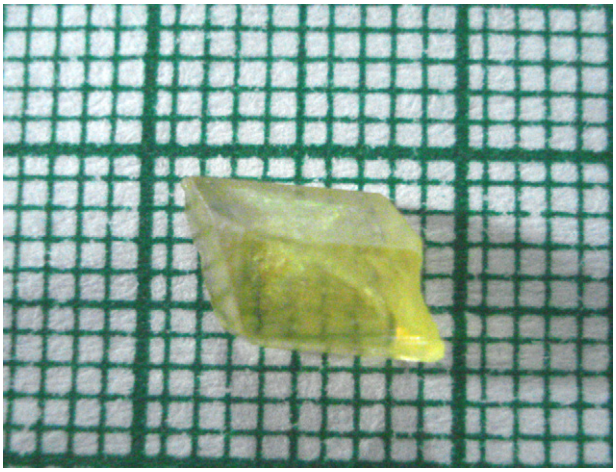

Fig. 1. Harvested CDMABA crystal.

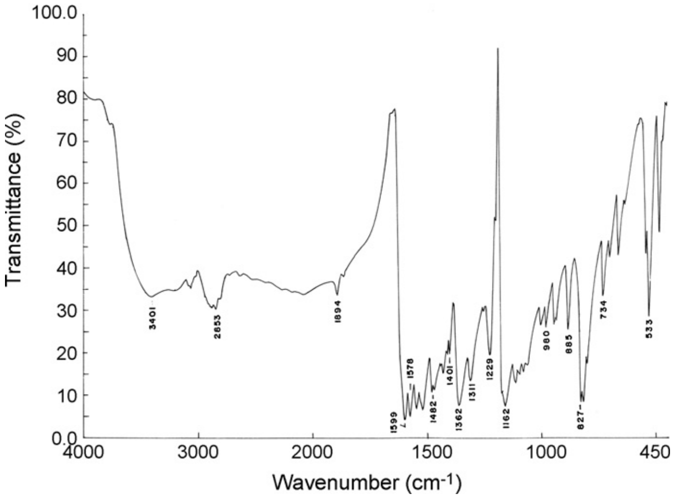

Fig. 2. FTIR spectrum of CDMABA.

aniline (p-ca) taken in equimolar ratio [12]. The reaction mixture was refluxed in ethanol about 8 h and the solution was filtered using Whatman filter paper and the resulting product of 4-chloro-4′dimethylamino-benzylidene aniline was obtained. The reaction mechanism is depicted in Scheme 1. Activated charcoal was added in solution at the hot condition for removing colored impurities. The purified product was shinny and yellow in color. The Thin Layer Chromatography (TLC) confirmed the yield of single compound of the synthesized material. Important factor that influences the habit of growing crystals is the polarity of the solvents [13]. Hence, in this study a few organic solvents were employed to identify the reasonable solvent. Table 1 presents the electric dipole moment of these solvents [14] and their influence on the growth habits of CDMABA crystal. The solubility of CDMABA in acetone was assessed as a function of temperature in the range of 20–40 °C. Single crystals of CDMABA were grown from saturated acetone solution of the synthesized salt by the slow evaporation technique at room temperature. During the slow evaporation, transparent crystal of dimension 8 mm × 5 mm × 4 mm was grown in a period of 16 days and is shown in Fig. 1.

3. Characterization

3.1. FTIR and FT-Raman spectral analyses

FTIR and FT-Raman spectral analyses were carried out to characterize the functional groups of the CDMABA crystal molecules [15]. FTIR spectrum was recorded for the purified sample using PerkinElmer- Paragon-500 by KBr pellet technique between 400 cm^{-1} and 4000 cm^{-1} and shown in Fig. 2. Benzylidene anilines display their C=N stretching as a band at 1600 cm^{-1} [16]. The band obtained at 1599 cm^{-1} is due to the formation of imine group (C=N) as a result of the condensation reaction between aldehyde and amine. C–H stretching absorption, a weak absorption, is observed at 3055 cm^{-1}. C=C stretching absorption is confirmed from the band at 1525 cm^{-1}. As para-di-substituted benzenes show C–H deformation vibrations in the region 840–800 cm^{-1} [16], the presence of C–H deformation is evident from the vibration at 827 cm^{-1}. Absence of characteristic aldehyde band at 2720 cm^{-1} indicates that there is no aldehyde group in the final product. The FT-Raman spectrum was recorded at 300 K using a Thermo Electron Corporation, USA spectrometer in the range of 100–3600 cm^{-1}. The FT-Raman spectrum also shows the presence of the functional groups in the crystal and shown in Fig. 3. The observed experimental values of FTIR and FT-Raman spectra were tabulated in Table 2.

Table 1
Effect of solvents on the growth habits of CDMABA crystal.

Solvents	Electric dipole moment (Debye)	Morphology	Visual quality
Benzene	0	Platelet	Good
Acetone	2.88	Prismatic	Good
Ethylacetate	1.78	Platelet	Good
Chloroform	1.04	Prismatic	Poor

3.2. NMR spectral analysis

In the present study, the proton NMR spectral analysis was made on the CDMABA crystal sample in deutrated $CdCl_3$ using in Bruker AC200–NMR Spectrometer. The Proton NMR spectrum of CDMABA (Fig. 4) shows six important absorption peaks namely,

Table 2
Important spectral band assignment of FTIR and FT-Raman lines of CDMABA.

Experimental wave number (cm^{-1})		Modes of vibration
FTIR	FT-Raman	
1599(s)	1596(s)	ν (C=N)
2853(m)	2988(s)	ν (N–CH_3) or (C–H)
1552(s)	1551.2(m)	ν (C=C)
1162(m)	1162.5(m)	ν (C–H)
827(s)	–	δ (C–H)

(s) strong; (m) medium; (ν) stretching; (δ) bending or deformation.

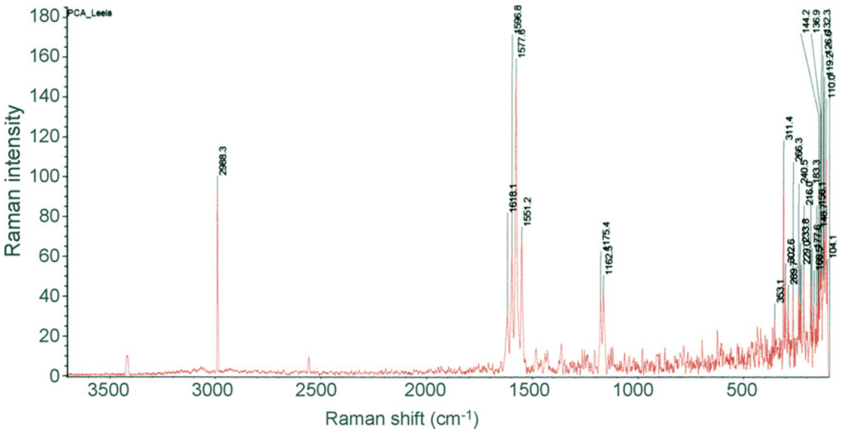

Fig. 3. FT-Raman spectrum of CDMABA.

A, B, C, D, E and F. They represent the hydrogen atoms present in five different chemical environments in the CDMABA molecule [17]. Different types of protons in different groups corresponding to peaks A, B, C, D, E and F are identified by the chemical shift (δ) values: one proton singlet (CH=N) = 8.2δ [A], two proton doublet ($H_a - H_{a'}$) = 6.7δ [B], two proton doublet ($H_b - H_{b'}$) = 7.7δ [C], the other two proton doublet ($H_c - H_{c'}$) = 7.1δ [D], two proton doublet ($H_d - H_{d'}$) = 7.3δ [E], and six singlet proton [$(CH_3)_2$] = 3.0δ [F]. The absorption peak A in the spectrum is a singlet, which corresponds to the C–H proton. This is because the number of proton present in the neighboring carbon is zero. Therefore, the splitting pattern is singlet at 8.2δ. In the NMR spectrum of CDMABA, the ratio of steps obtained are, $A{:}B{:}C{:}D{:}E{:}F$ = 1:2:2:2:2:6. Thus, the numbers of protons associated with the signals are: A, 1H; B, 2H; C, 2H; D, 2H; E, 2H; F, 6H, respectively; thus confirming the formation of CDMABA.

3.3. Single crystal and powder XRD

The powder X-ray diffraction pattern was recorded using powder X-ray diffractometer with CuKα_1 radiation (λ = 1.54060 Å). Finely crushed powder of CDMABA crystal was scanned in the 2θ values ranging from 10 to 70°. The obtained peaks were indexed and are shown in Fig. 5. Single crystal XRD studies show that the crystal belongs to monoclinic system with cell parameters of a = 9.599 Å, b = 16.417 Å, c = 9.764 Å and β = 119.17°. The morphology and the crystallographic planes of the CDMABA crystal are indexed from single crystal XRD and are shown in Fig. 6.

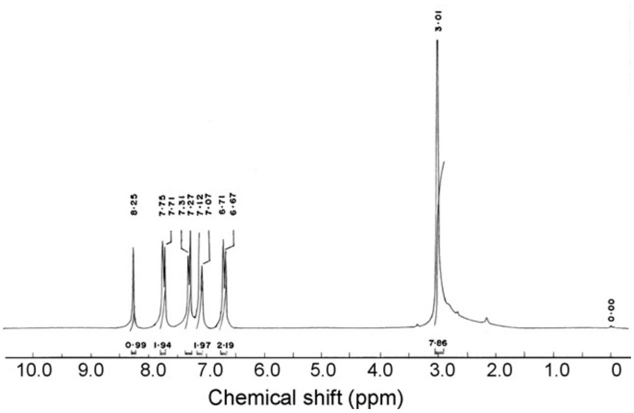

Fig. 4. ^{1}H-NMR spectrum of CDMABA.

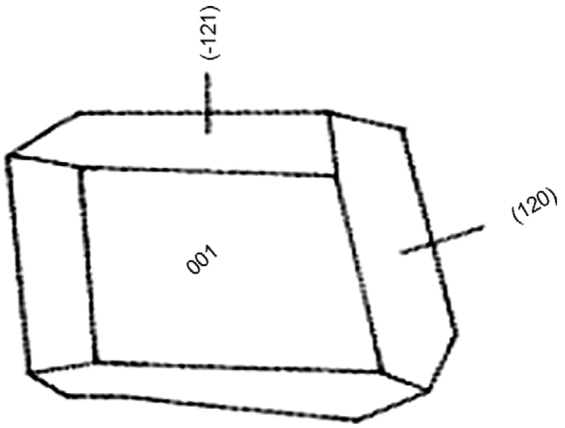

Fig. 5. Morphology of the CDMABA crystal.

3.4. High resolution X-ray diffraction analysis

The study on the grown crystal to ascertain its quality has significant importance for device fabrication. The defects created during growth have severe consequences on the physical properties of the crystal. Hence studies to reveal the quality of the grown crystals are important. In this work the degree of crystalline perfection of CDMABA was obtained by recording high resolution X-ray diffraction (HRXRD) curves. A multicrystal X-ray diffractometry (MCD) [18] developed at National Physical Laboratory (NPL), New Delhi, was used to study the quality of the solution grown CDMABA sin-

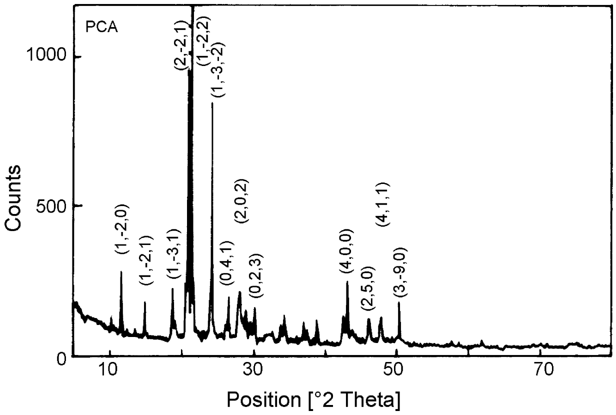

Fig. 6. Powder XRD pattern of CDMABA.

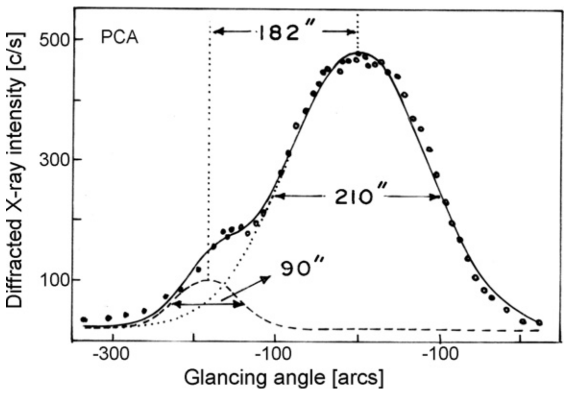

Fig. 7. HRXRD spectrum of CDMABA.

gle crystal. Before recording the diffraction curve, to remove the non-crystallized solute atoms remained on the surface of the crystal and also to ensure the surface planarity, the specimen was first lapped and chemically etched in a non-preferential etchant of water and acetone mixture in 1:2 volume ratios. This process also ensures to get rid from surface layers, which may some times form a complexating epilayer on the surface of the crystal due to organic additives [19]. Fig. 7 shows the high-resolution diffraction curve (DC) recorded for a typical CDMABA specimen using MoKα_1 radiation (0.70926 Å) in symmetrical Bragg geometry of the multicrystal X-ray diffractometer. The diffracting plane chosen to record the DC was ($2\,\bar{2}\,1$). As seen in Fig. 7, the curve does not contain a single diffraction peak. The solid line, which follows well with the experimental points (filled circles), is the convoluted curve of two peaks using the Lorentzian fit. The additional peak depicts an internal structural low angle (tilt angle $\alpha > 1$ arc min but less than a deg.) grain boundary [19] whose tilt angle (misorientation angle between the two crystalline regions on both sides of the structural grain boundary) is 182 arc s from its adjoining region. The Full Width Half Maximum (FWHM) of the main peak and the very low angle boundary are respectively 210 and 90 arc s. Though the crystal contains a low angle boundary, the relatively low angular spread of around 500 arc s of the DC shows that the crystalline perfection is fairly good [18,19].

3.5. *Linear and nonlinear optical properties*

In order to estimate the optical transparency in the 200–1200 nm region of the electromagnetic spectrum, the optical transmittance study was carried out on the CDMABA crystal of thickness ~0.2 mm employing Shimadzu 1601 model spectrophotometer. In this study the transmittance of the sample, which is the descriptive of the result of absorption processes, was recorded at room temperature. π–π^* transition occurs at 280 nm due to the C=N (imine group) bond. The lower cutoff wavelength of the CDMABA is at about 367 nm (Fig. 8) and the crystal is transparent in the entire visible and near infrared region.

3.6. *Z-scan technique*

In present case, we choose to work at 632.8 nm in order to evaluate materials at visible wavelengths in which there exist interest for switchable holographic filters and refractive optical limiters [5]. Hence the Z-scan method has gained rapid acceptance by the nonlinear optics community as a standard technique for separately determining the nonlinear changes in refractive index and change in optical absorption. Sheik-Bahae et al. [20] and Vanstryland and Sheik-Bahea [21] have reported a single beam method for measuring the sign and magnitude of nonlinear refractive index (n_2) that has the sensitivity compared to interferametric methods. Using a single Gaussian laser beam in tight focus geometry, as depicted in Fig. 9, the transmittance of a nonlinear medium through a finite aperture in the far field as a function of the sample position *Z* can be measured with respect to the focal plane. The nonlinear absorption and refractive index of CDMABA crystals (thickness ≈3 mm) were estimated using the single beam Z-scan method with CW laser beam intensity of 15 mW and the wavelength of 632.8 nm. The study of nonlinear refraction by the Z-scan method depends on the position (*Z*) of the thin samples under the investigation along a focused Gaussian laser beam. The sample causes an additional focusing or defocusing, depending on whether nonlinear refraction is positive or negative. In the most reported experiments, $0.1 < S$ (transmittance) <0.5 has been used for determining nonlinear refraction. Obviously, the $S = 1$ corresponds to the collection of all transmitted light and therefore is insensitive to any nonlinear beam distortion due to nonlinear refraction [22]. Such a scheme, referred to as an "Open aperture" Z-scan, is suited for measuring nonlinear absorption in the sample. Results obtained from a typical closed aperture Z-scan study for the grown CDMABA are presented in Fig. 10. The nonlinear refractive index (n_2) of the crystal was calculated using the standard relations given below [20–22]:

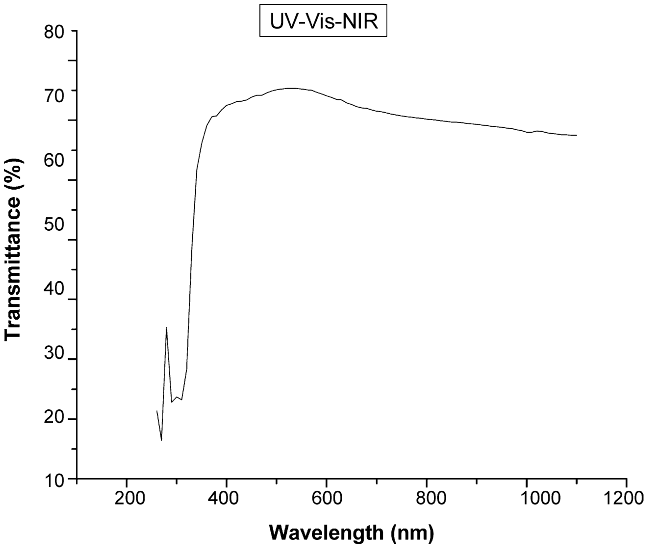

Fig. 8. UV–vis–NIR spectrum of CDMABA.

$$\Delta T_{P-V} = \frac{0.406(1-S)0.25^{*}}{\Delta\phi_0} \tag{1}$$

where ΔT_{P-V} is the difference between the normalized peak and valley transmittance, $\Delta T_{P-V}/\Delta\phi_0$ is the on-axis phase shift at the focus, *S* is the linear transmittance of the aperture. The nonlinear refractive index (n_2) and nonlinear absorption coefficient (β) are given by,

$$n_2 \approx \frac{\Delta\phi_0}{kI_0L_{\text{eff}}} \tag{2}$$

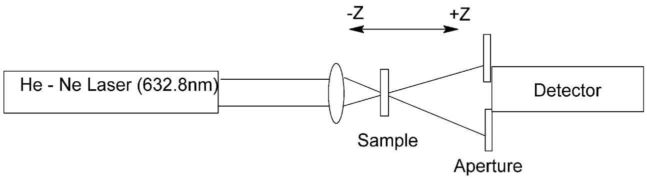

Fig. 9. Experimental setup for the Z-scan measurements.

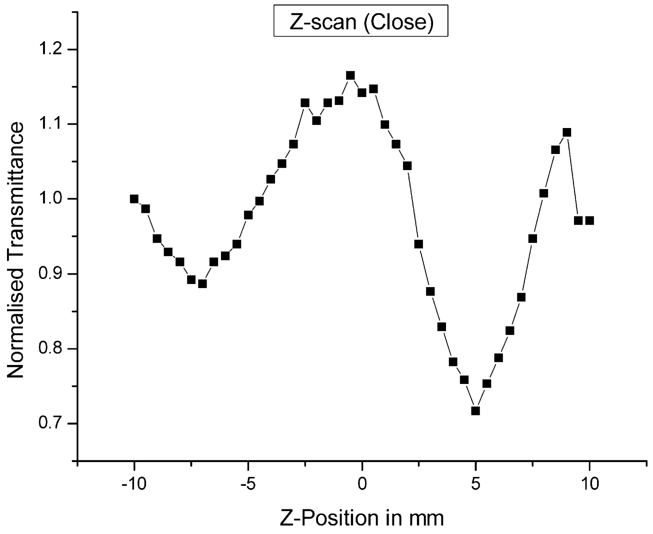

Fig. 10. Z-scan (close) spectrum of CDMABA.

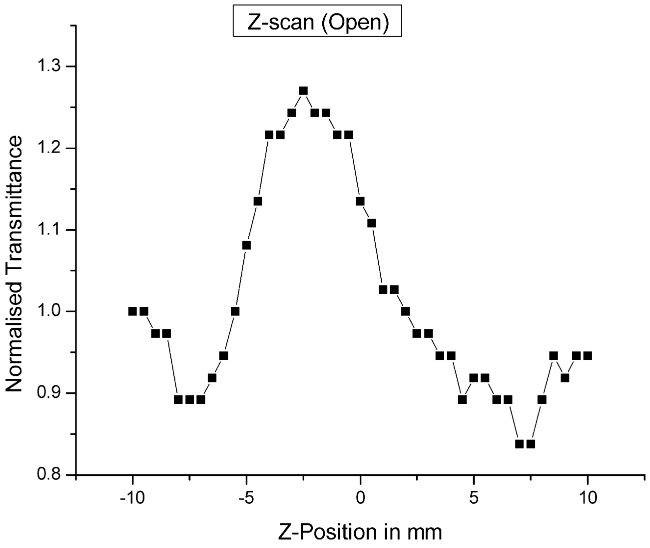

Fig. 11. Z-scan (open) spectrum of CDMABA.

and

$$\beta = \frac{2\sqrt{2}\Delta T}{I_0 L_{\mathrm{eff}}} \tag{3}$$

where k is the wave number ($k = 2\pi/\lambda$), and $L_{\mathrm{eff}} = [1 - \exp(-\alpha L)]/\alpha$ with $I_0 = P/(\pi\omega_0^2)$ defined as the peak intensity within the sample, where L is the thickness of the sample, and α is the linear absorption coefficient. The ratio of the signals with and without the aperture accounts for the nonlinear absorption and gives the information about purely nonlinear refraction. The enhanced transmission near the focus is indicative of the saturation of absorption at high intensity. Absorption saturation in the sample enhances the peak and decreases the valley in the closed aperture Z-scan. The focusing effect is attributed to a thermal nonlinearity resulting from absorption of radiation at 632.8 nm. Localized absorption of a tightly focused beam propagating through an absorbing medium produces a spatial distribution of temperature in the crystal and, consequently, a spatial variation of the refractive index that acts as a thermal lens resulting in phase distortion of the propagating beam (Fig. 10). The nonlinear absorption property of the D–π- A type π-electron system can be related closely to the π-electron conjugate degree and delocalization capacity of the molecule. The three dimensional X-ray crystal structure solution of this crystal showed that the torsion angles C8–N1–C7–C1 = 179.93(13)°, C15–N2–C4–C5 = 179.36(18)° and C15–N2–C4–C3 = 0.1(3)°, in these conjugated chains, are coplanar [12]. These are all favourable to nonlinear optical absorption, especially to saturated absorption. Nonlinear refractive index (n_2) of the CDMABA calculated is 5.8107×10^{-7} cm^2/W the value of nonlinear absorption coefficient (β) (Fig. 11) estimated from the open Z-scan curve is 0.1854 cm/W.

3.7. Thermal analysis

Thermogram and differential thermogram analyses on CDMABA were carried out using STA 409PC. Thermogravimetric (TG) and differential thermal analysis (DTA) of CDMABA recorded at a heating rate of 10 K/min under nitrogen atmosphere is shown in Fig. 12. Thermal Gravimetric Analysis (TGA) curve shows that there is no weight loss between 100 °C and 200 °C. This indicates that there is no inclusion of water in the crystal lattice. As there is no weight loss before melting point, the material is moisture-free and stable upto 152 °C. The final residue weight is 1.26%. From the DTA curve it is observed that the material is stable up to 152.9 °C, the melting point of the substance and it undergoes irreversible endothermic transition at 799 °C. The melting point of the substance measured using 'GUNA make' melting point apparatus was 150–153 °C. TGA curve shows that there is a sharp weight loss at 361 °C and sample undergoes gradual weight loss till 800 °C. Differential scanning calorimetry (DSC) study performed for the grown CDMABA using NETZSCH-Geratebau GmbH Thermal analysis (STA 409PC) in the temperature range 27–250 °C at a heating rate of 10 K/min in the Nitrogen atmosphere is shown in Fig. 13. 10.500 mg of sample was placed in the Alumina crucible. The crystal of CDMABA is stable up to its melting point (152 °C). The sharpness of the peak confirms the good crystallinity of the synthesized compound [23].

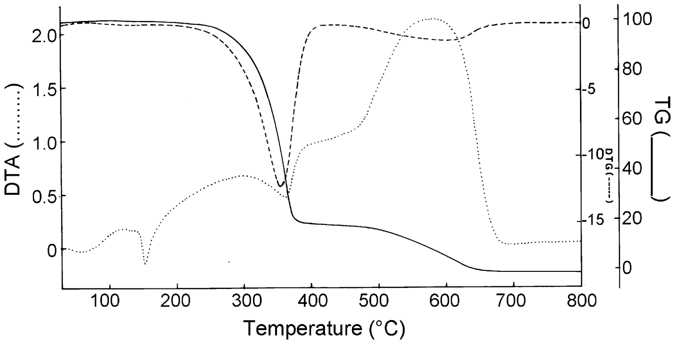

Fig. 12. TGA/DTA spectrum of CDMABA.

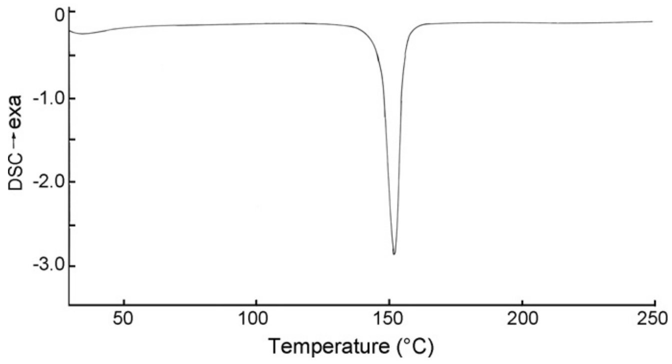

Fig. 13. DSC spectrum of CDMABA.

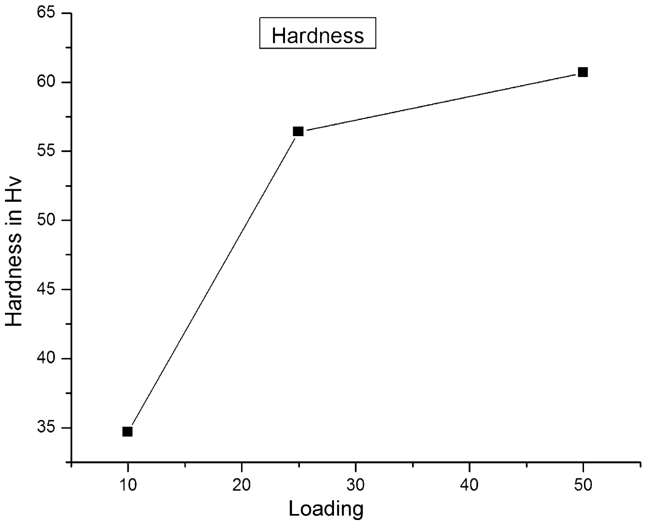

Fig. 14. Microhardness values vs. load for CDMABA crystal on (0 0 1).

3.8. Hardness

Microhardness testing is one of the best methods for understanding the mechanical properties of materials [24]. The mechanical strength of the CDMABA crystal was measured using a HMU microhardness tester fitted with a diamond indenter attached to HMU incident light microscope. Indentations were made for various loads from 10 g to 50 g. Several trials of indentation were carried out on the prominent (0 0 1) face and the average diagonal length was calculated for an indentation time of 8 s. The Vickers hardness number (H_V) of the crystal was calculated using the relation $H_V = 1.8544\,P/d^2$, where P is the applied load in kg and d is the average diagonal length of impression in mm. Fig. 14 shows the variation of H_V with load for CDMABA. Cracks were observed for loads more than 50 g.

4. Conclusion

Optical quality single crystals of CDMABA were grown at room temperature using the solution growth technique. The morphology unveils the growth habits of the material. The UV–vis–NIR spectrum elucidates that the crystal is transparent between 360 nm and 1200 nm. From the FTIR, FT-Raman and NMR spectrum, the formation of the imine group of the material was confirmed. Thermal analyses indicate that the crystal has good thermal stability. A sharp peak observed at 150 °C in the DSC curve corresponds to the melting point of the material. The microhardness study revealed that the crystal develops cracks for load more than 50 g. High Resolution X-ray Diffraction study shows that the perfection of the crystal is fair even though it contains a low angle boundary. The relative third order nonlinear optical absorption and the nonlinear optical refractive index were calculated by the Z-scan technique.

Acknowledgment

One of the authors (SL) thanks to Dr. A. Ilangovan, School of Chemistry, Bharathidasan University, Tiruchirappalli for fruitful discussion and Dr. Sastikumar, Professor and Head, NIT, Tiruchirappalli for his permission to utilize the facilities available at the Optics Laboratory. Further the authors thank University Grant Commission, Government of India for financial assistance [File No. 3237/2007 (SR)].

References

[1] E.W. Van Stryland, H. Vanherzeele, M.A. Woodall, M.J. Soileau, A.L. Smirl, S. Guha, T.F. Bogess, Opt. Eng. 24 (1985) 613.
[2] M. Sheik-Bahae, A.A. Said, T. Wei, D.J. Hagan, E.W. Van Stryland, IEEE J. Quantum Electron. 26 (1990) 760–769.
[3] J.J. Rodrigues Jr., L. Misoguti, F.D.C.R. Nunes Mendonca, S.C. Zilio, Opt. Mater. 22 (2003) 235–240.
[4] M. Somac, A. Somac, B.L. Davies, M.G. Humphery, M.S. Wong, Opt. Mater. 21 (2002) 485–488.
[5] L.V. Natarajan, R.L. Sutherland, V.P. Tondiaglia, T.J. Bunning, W.W. Adams, J. Nonlinear Opt. Phys. Mater. 5 (1996) 89–98.
[6] X. Xu, W. Qiu, Q. Zhou, J. Tang, F. Yang, Z. Sun, P. Audebert, J. Phys. Chem. B (Article) 112 (16) (2008) 4913–4917.
[7] J.G. Breitzar, D.D. Diott, L.K. Iwaki, S.M. Kirkpatrick, T.B. Rauchturs, J. Phys. Chem. A 103 (1999) 6930–6937.
[8] W. Yu, L. Yang, T.L. Zhang, J.G. Zhang, F.J. Ren, Y.H. Liu, R.F. Wu, J.Y. Guo, J. Mol. Struct. 794 (2006) 255–260.
[9] K. Srinivasan, R. Biravaganesh, R. Gandhimathi, P. Ramasamy, J. Cryst. Growth 236 (2002) 381–392.
[10] N. Azariah, A.S.H. Hameed, T. Thennappan, M. Noel, G. Ravi, Mater. Chem. Phys. 88 (2004) 90–96.
[11] S. Leela, K. Ramamurthi, H.S. Evans, G. Vasuki, Acta Crystallogr. E 63 (2007) o4805.
[12] X.L. You, C.R. Lu, Y. Zhang, D.C. Zhang, Acta Crystallogr. C 60 (2004) o693–o695.
[13] K. Udayalakshmi, K. Ramamurthi, Cryst. Res. Technol. 40 (2005) 1165–1168.
[14] R.L. David (Ed.), CRC Handbook of Chemistry and Physics, 15, 80th edition, CRC Press, LLC, 1999–2000, p. 14.
[15] P. Kalsi, Spectroscopy of Organic Compounds, Wiley Eastern, New Delhi, 1985.
[16] W. Kemp, Organic Spectroscopy, 3rd edition, ELBS, Macmillan, 1993.
[17] Y.R. Sharma, Elementary Organic Spectroscopy, S. Chand, New Delhi, 2000.
[18] G. Bhagavannarayana, S. Parthiban, Subbiah Meenakshisundaram, J. Appl. Cryst. 39 (2006) 784–790.
[19] G. Bhagavannarayana, R.V. Ananthamurthy, G.C. Budakoti, B. Kumar, K.S. Bartwal, J. Appl. Cryst. 38 (2005) 768–771.
[20] M. Sheik-Bahae, A.A. Said, E.W. VanStryland, Opt. Lett. 14 (1989) 955–957.
[21] E.W. Vanstryland, M. Sheik-Bahae, in: M.G. Kuzyk, C.W. Dirk (Eds.), Characterisation Techniques and Tabulation for Organic Nonlinear Materials, Marcel Dekker Inc., 1998, pp. 655–692.
[22] T. Kanagasekaran, P. Mythili, P. Srinivasan, A.Y. Nooraldeen, P.K. Palanisamy, R. Gopalakrishnan, Cryst. Growth Des. 8 (2008) 2335–2339.
[23] H.H. Willard, L.L. Merritt Jr, J.A. Dean, F.A. Settle, Instrumental Methods of Analysis, Wadsworth Publishing Company, USA, 1986, p. 609.
[24] B. Lal, K.K. Bamzai, P.N. Kotru, Mater. Chem. Phys. 78 (2003) 202–207.